Carbohydrate Polymers **18** (1992) 243-251

Gelation of xanthan with trivalent metal ions

Heike Nolte,[a]* Sabine John,[a]‡ Olav Smidsrød[b] & Bjørn T. Stokke[a]

[a] *Department of Physics and Mathematics,* [b] *Division of Biotechnology, Norwegian Biopolymer Laboratory, University of Trondheim, NTH, N-7034 Trondheim, Norway*

(Received 10 July 1991; revised version received 20 September 1991; accepted 25 September 1991)

In-situ gelation of semidilute xanthan solutions with trivalent chromium, aluminum or iron ions was studied by rheology and UV-spectroscopy. Measurements of the elastic modulus of xanthan gel cylinders prepared by dialysis against the complexing ion at pH values from 2 to 6 indicate that monomeric species of the ion are ineffective, whereas dimeric or higher oligomeric species are effective in crosslinking the polysaccharide. When chromium was used as the crosslinking species, the dependence of the gelation rate on the ionic concentration followed a power law with a coefficient of 1·7. The gelation time and the gelation rate were found to extrapolate to zero at 1 mM Cr for 2·5 mg/ml xanthan. The limiting concentration of xanthan needed for gelation with 5 mM Cr(III) at 20 °C was estimated as 0·35 mg/ml. This critical xanthan concentration is close to the overlap concentration c^* estimated from the experimentally determined intrinsic viscosity $[\eta]$ using $c^* = 1{\cdot}4/[\eta]$. An apparent activation energy for crosslinking of xanthan was calculated as $E_a = 42$ kJ/mol and $E_a = 108$ kJ/mol for Cr and Al ions, respectively. The fractal dimensionality of xanthan–Cr at the sol–gel transition was estimated as 1·3 applying the Chambon–Winter criterion for gelation, thus indicating that this gelation criterion is applicable also to stiff-chain polysaccharides such as xanthan.

INTRODUCTION

Gel technology based on ionic crosslinked polysaccharides is currently in use and of considerable interest for potential application in the oil industry. The applications range from rheological control in hydraulic fracturing operations, to delaying the reaction between acid and carbonate in an acid fracturing process, and to permeability modification of heterogeneous reservoirs in order to avoid water-channeling in high-permeable zones (Menjivar, 1986; Moradi-Araghi *et al.*, 1988; Borchardt, 1989). The last application is also referred to as profile control or profile modification for near-wellbore treatments extending 15–30 m into the formation from the injection well, and in-depth treatment involving placement of gels up to 100 m from the injection well. The challenge of an in-depth treatment operation is to obtain gelation times of the order of weeks under reservoir conditions (Moradi-Araghi *et al.*, 1988). Various polysaccharides, e.g. guar, xanthan and welan, and crosslinking ions, e.g. Cr^{3+} and Al^{3+}, have been proposed and evaluated in laboratory bulk and model porous media studies (Conway *et al.*, 1983; Prud'homme & Uhl, 1984; Menjivar, 1986; Hubbard *et al.*, 1986; Hejri *et al.*, 1989).

In a previous communication, the authors reported the effects of polymer and ion concentration on the sol-gel transition of xanthan-Cr(III) using dynamic-oscillatory measurements at one selected frequency. The studies were carried out at $T = 20$ °C and at pH 3·5 (Lund *et al.*, 1988). In this study, the authors extend the experimental parameters to include effects of temperature and pH in solution. The motivation for including the pH as an experimental parameter is a study by Shu (1989) who reported that the pH of the chromium solution has a dominant impact on the gelation kinetics of xanthan. This is due to the relative abundance of different chromium species which differ in crosslinking efficiency at various pH values (Baes & Mesmer, 1976). Likewise, a similar effect of pH on the efficiency of Cr^{3+} on crosslinking polyacrylamide has recently been reported (Burrafato *et al.*, 1990). The temperature dependence of the gelation rate has

---

*Present address: Deutsches Wollforschungsinstitut, der Rheinisch-Westfälischen Technischen Hochschule Aachen, Veltmanplatz 8, D-5100 Aachen, FRG.

‡Present address: Grace GmbH, In der Hollerhecke 1, D-6520 Worms, FRG.

practical value because there are temperature differences between the injection fluids and the reservoir, and, in addition, it can be used to estimate an apparent activation energy for the crosslinking reaction.

The techniques used in this study were extended from the dynamic-oscillatory shear rheology at one fixed frequency used previously (Lund *et al.*, 1988) to include frequency scans at selected intervals. This was undertaken to be able to test the applicability of the Chambon–Winter criterion (Chambon & Winter, 1985, 1987; Winter & Chambon, 1986) for the sol–gel transition, i.e. that the ratio between the loss and storage modulus, $G''(\omega)/G'(\omega)$, is independent of the excitation frequency, ω, at the gel point. The actual value of G''/G' thus observed depends on the fractal dimensionality, d_f, at the gel point, the critical gel. The fractal dimensionality d_f was estimated as $1{\cdot}5 \pm 0{\cdot}05$ for agar gels (Burchard & Ross-Murphy, 1990), which was a decrease from 1·78 estimated for agar dispersed in solution. Whether physically crosslinked stiff-chain polysaccharides like double-helical xanthan (Sato *et al.*, 1984*a*,*b*; Atkins, 1990) also conform to this formalism is therefore of interest. Complementary information to the rheological characterization was obtained by difference absorption spectroscopy of the xanthan–Cr(III) solution relative to that of the components. The aim of this paper was to obtain information on the crosslink density in the gel utilizing a low molecular weight model compound in the ligand-exchange reaction in the hydration shell of chromium as a calibration. The correlation between crosslink density and the rheological properties was of particular interest.

MATERIALS AND METHODS

Materials

Xanthan obtained as a fermentation broth (Biosentrum Statoil, Stavanger, Norway) at a polymer concentration of about 40 mg/ml was utilized in all experiments except for the gel-volume studies in various solvents. Low molecular weight substances remaining in the fermentation broth may influence the kinetics of gel formation, and the polymer samples were therefore purified by the following procedure: the xanthan stock solution was diluted with 0·1 M NaCl to a concentration of approximately 2·5 mg/ml and filtrated under high pressure. The polymer was subsequently precipitated with two volumes of iso-propanol, washed with iso-propanol and dried. Solutions for rheological characterization were made by dissolving the required weight of xanthan in 0·1 M NaCl and stirring at room temperature overnight. The intrinsic viscosity, $[\eta]$, of the purified sample was determined using a Cartesian diver viscometer designed essentially as described by Troll *et al.* (1980), to be 4100 ± 300 ml/g at $T = 20{\cdot}1\,°C$. Xanthan solutions with a relative viscosity η_{rel} less than 2·0, and a shear rate $\dot{\gamma}$ from 2·42/s to 17·45/s were studied. A slight decrease in $[\eta]$ was observed at the highest shear rates studied, and the given value was obtained at the low shear rate plateau. Xanthan with the trade name Kelzan XCD (Kelco Inc., A Division Merck, San Diego, CA, USA) was used for forming the gel beads. The powdered sample was dissolved in water overnight and removal of insoluble material consisting of higher molecular weight aggregates (Lund *et al.*, 1988) was found not to influence the measured elasticity of the xanthan–Cr(III) gel beads.

The metal salt solutions were prepared by dissolving $Me(NO_3)_3 \cdot 9H_2O$ (Me = Cr, Al, Fe) (Merck, Darmstadt, FRG) in distilled water. The desired pH values of the solutions were obtained by adding aqueous NaOH or aqueous HCl dropwise.

Determination of elastic modulus of xanthan–gel cylinders

Experiments studying the effect of pH were carried out on gel cylinders. Gel cylinders were made by filling the xanthan dissolved in 0·1 M NaCl solutions at the desired concentration in cylindrical tubes (diameter $(D) = 14$ mm, $L = 19$ mm), capping them with dialysis membrane and immersing them in an excessive volume of the gel-inducing electrolyte at the desired concentration and pH. The gel was formed by diffusion of the metal ions through the dialysis membrane for a total of 72 h with change of electrolyte every 24 h. The elastic modulus of the gel cylinders was determined at 1 mm uniaxial compression at a deformation rate of 0·2 mm/s using a Stevens Texture Analyzer. The values reported reflect the average of three gel cylinders.

Xanthan gel beads

Xanthan gel beads for studying relative gel volume changes in different solvents were made as previously described for Ca-alginate gel beads (Martinsen *et al.*, 1989) by dripping 10 mg/ml unbuffered xanthan (Kelzan XCD) solution into 100 mM $Cr(NO_3)_3$, pH adjusted to 3·4 and $T = 45\,°C$.

Rheological characterization *in situ*

The in-situ gelation experiments were performed using a gravitational pendulum rheometer (Mikkelsen *et al.*, 1986). The computerized instrument equipped with a specific pendulum–ceuvette combination was calibrated using glycerol solutions with viscosities ranging from 3 to 20 mPa s determined with a Ubbelhode capillary viscometer. The pendulum–cuvette combination used in the experiments was calibrated to have an instrument parameter $C = 0{\cdot}95$ Pa. The temperature was controlled by circulating water in the rheometer walls using a Haake DG 8 thermostat.

Aliquots of 5 ml of the polysaccharide and the metal ion solution were equilibrated to the actual temperature, subsequently mixed and immediately filled into the rheometer cuvette. Experimental determination of the storage (G') and loss moduli (G'') were then started. The gelation time refers to the time after combining the two solutions. For the experiments above $T = 20\,°C$ the gelling sample was covered with a thin paraffin oil layer to prevent evaporation. The measurements were repeated, automatically controlled, after certain time intervals using an excitation frequency range ($\omega = 0{\cdot}157$–$6{\cdot}4$/s). Rheological characterizations were carried out at small deformations, $\gamma < 0{\cdot}01$, corresponding to the linear viscoelastic regime. Parallel experiments at maximum deformations of 0·006 and 0·009 in oscillation revealed no effect on the kinetics of gelation. Likewise, decreasing the number of frequency scans from two to one per hour did not affect the kinetics of gelation.

Spectroscopical measurements

Dispersion UV-spectra were obtained using a Shimadzu UV-260, and the change in UV-absorption as a function of time was recorded employing a Zeiss PMQ3. The gels were prepared directly in the sample cuvette. All spectra were measured by using the corresponding solutions simultaneously, but separately, as references. The absorption refers to a path length of 1 cm unless otherwise stated.

RESULTS AND DISCUSSION

Elasticity of gel cylinders

Figure 1 shows the modulus of elasticity E of 1% xanthan–50 mM Me^{3+} (Me = Fe,Al,Cr) cylindrical gels versus the pH of the dialysis solution. Cr(III) and Al(III) induced gelation within nearly the same pH range from 3·0 to 5·0, whereas the Cr(III) gels showed higher elasticity than the Al(III) gels. Only Fe(III) formed gels with xanthan at pH values < 2·6. We observe a maximum in the gel strength versus the pH for Al and Fe, whereas for Cr there is a monotonic increase in elasticity within this pH range. Dialysis of xanthan against aqueous Cr(III) at pH 6 did not yield a gel. This suggests that there is an optimum in elasticity versus pH also for xanthan–Cr gels.

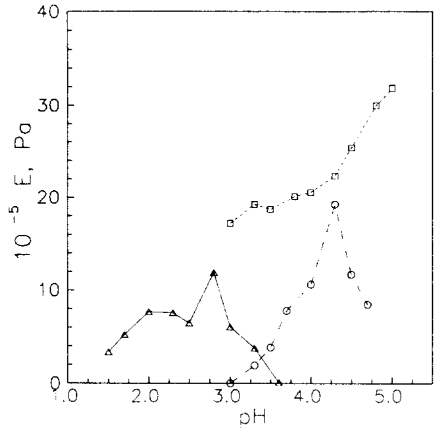

Fig. 1. Modulus of elasticity E of 10 mg/ml xanthan gel cylinders versus pH in metal ion solutions for 50 mM $Al(NO_3)_3$ (○), 50 mM $Fe(NO_3)_3$ (△) and 50 mM $Cr(NO_3)_3$ (□).

The optimum in elasticity and the lower and upper pH limits of gelation can be related to the hydration of the metal ions. The metal ions employed are able to form dimeric, trimeric and higher oligomers depending on the pH in solution (Baes & Mesmer, 1976). The lower limits in pH where gels are observed to occur are associated with the formation of dimeric species of the hydrated ions and the ionization of the carboxylic group. The pK_a value of xanthan in 0·1–0·2 M NaCl is reported to be 2·6 (Holzwarth, 1976; Zhang *et al.*, 1987). Increasing the pH yields higher oligomers by an olate mechanism, and the average number of ions involved in the cluster increases with pH. The upper limit where gelation is observed using the dialysis method is related to the formation of even larger clusters. For instance, the insoluble trihydroxide $[Cr(OH)_3(H_2O)_3]_n$ is the stable state of the trivalent chromium ion above pH 6 (Baes & Mesmer, 1976). This results in a pH dependent crosslink density yielding an optimum in gel strength versus pH for all three metal ions. The decrease in E observed at the high end of the pH range investigated could either be due to the decreasing crosslinker concentration or the dialysis method used, since the oligomeric olates of the metal ions might be of similar size to the pores in the dialysis membrane. This could reduce the diffusibility of the crosslinker through the pores of the dialysis membrane. Xanthan-Cr gel cylinders were found to be inhomogeneous, as reported for ionotropic gels of alginate and pectate made by the same dialysis method (Skjåk-Bræk *et al.*, 1989). This suggests that gelation close to the dialysis membrane can further reduce the diffusibility of crosslinking ions into the gel. A noteworthy finding is that the optimum in pH depends on the type of metal ion, and that this optimum is closely related to the reported formation of dimeric or higher oligomeric olates of the ions in solution.

Swelling equilibria

Changes in gel volume of polymeric gels exposed to solvent conditions different from those used during gelation has practical relevance to profile modification applications. Syneresis over long time, may impair the gel treatment and thus reduce the effective lifetime.

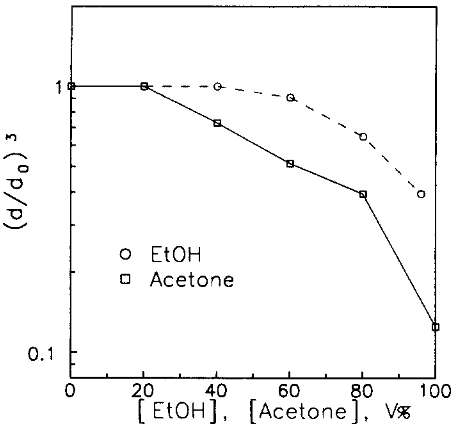

Fig. 2. Relative volume reduction $(d/d_0)^3$ of 0·5% xanthan-100 mM $Cr(NO_3)_3$ gel beads versus weight fraction of ethanol (○) and acetone (□) in water.

Figure 2 shows the relative volume reduction $(d/d_0)^3$ of 0·5% xanthan-100 mM $Cr(NO_3)_3$ gel beads for various compositions of ethanol and acetone-water solvents. The parameters d_0 and d are the gel bead diameter observed in the reference solvent (water) and the actual solvent, respectively. A significant reduction in gel bead volume was observed with increasing levels of ethanol or acetone, the volume decrease being largest for acetone. Similar experiments using NaCl from 1 mM to 6 M and HCl from 10 mM to 6 M revealed no significant changes in the xanthan gel bead volume. A minor effect on $(d/d_0)^3$ of xanthan and $Cr(NO_3)_3$ concentrations used during gel formation were observed. The intensity of the xanthan gel bead volume to the supporting electrolyte concentration is not unexpected for the stiff double-helical xanthan chain with a persistence length of about 120 nm (Sato *et al.*, 1984*a,b*).

Kinetics of xanthan–chromium gelation

Measurements of $G'(\omega,t)$ and $G''(\omega,t)$ at $\omega = 0{\cdot}157$/s during the crosslinking of xanthan with chromic ions give results in agreement with the authors' previous observations (Lund *et al.*, 1988). The viscous behavior dominates ($G'' > G'$) in the initial stage, whereas both G' and G'' increase as the gelation proceeds. The storage modulus rises more sharply than the loss modulus as the reaction proceeds, and G' predominates over G'' ($G' > G''$) towards the end of gelation. The crossover point, when G' is equal to G'', characterizes the sol–gel transition. Further information of the changes in the mechanical properties is obtained from the change in frequency dependence. The loss modulus nearly retains its dependence on ω over the entire time period, whereas a decrease in d $\log G'$/d $\log\omega$ is observed (Fig. 3(a)). The storage modulus is almost independent of ω which is characteristic of a viscoelastic solid, one day after initiation of the crosslinking reaction.

When the same data are presented as the loss tangent, $\tan\delta = G''/G'$, versus the reaction time at various frequencies (Fig. 3(b)), $\tan\delta$ at the lower ω depends more strongly on the reaction time than $\tan\delta$ at the higher ω, thus resulting in a crossover at a certain reaction time. This crossover is the gelation criterion according to Chambon and Winter (Chambon & Winter, 1985, 1987; Winter & Chambon, 1986) and is observed at $t = 3$ h under the given conditions (Fig. 3(b)). The actual value of $\tan\delta$ at this gelation threshold, $\tan\delta_G$, is related to the relaxation exponent n:

$$\tan\delta_G = \tan\left(\frac{n\pi}{2}\right) \qquad (1)$$

The relaxation exponent n is estimated as $n = 0{\cdot}35 \pm 0{\cdot}04$ from the data in Fig. 3(b). This observed relaxation

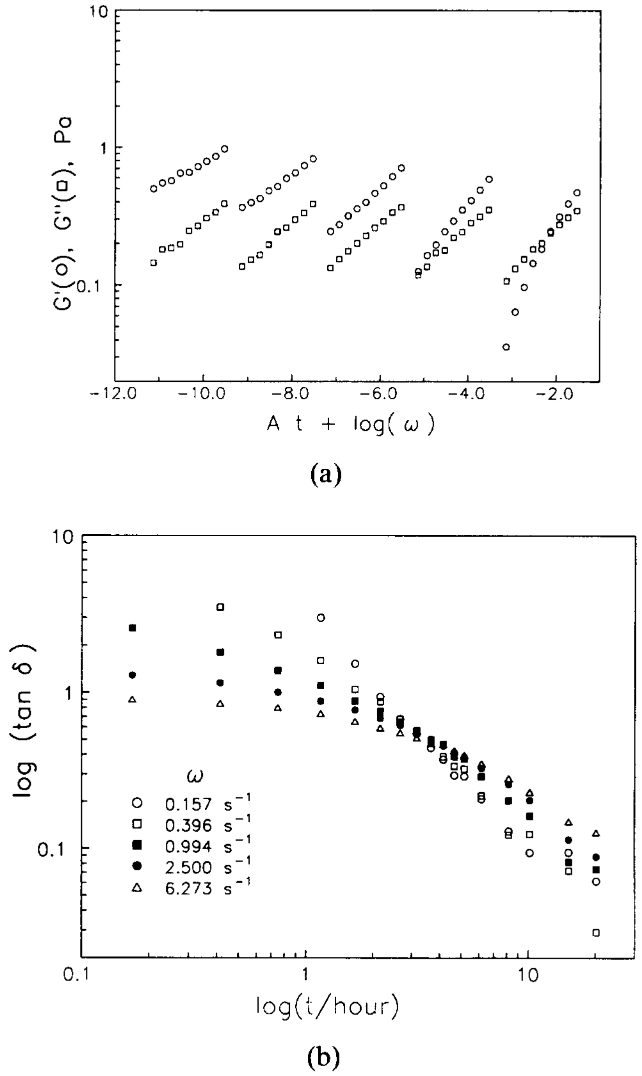

(a)

(b)

Fig. 3. (a) Storage modulus $G'(\omega)$ and $G''(\omega)$ versus frequency for a 2·50 mg/ml xanthan, 5 mM $Cr(NO_3)_3$ chromium solution at pH 3·4, $T = 20\,°C$, at different times after mixing. The G' and G'' at each frequency scan is shifted according to the time after mixing of the xanthan and chromium solution ($A = -2$ when t is in hours). (b) Loss tangent of the gelling solution in (a) versus reaction time at various angular frequencies.

exponent is in the low end of the range (0·18–0·7) of other chemically and physically gelled polymers (see compilation by Scanlan and Winter (1991)). Further insight into the observed relaxation exponent can be obtained from the calculable fractal dimensionality of the molecular cluster, d_f, at the gelation threshold:

$$M \sim R^{d_f} \tag{2}$$

where M and R are the molecular weight and physical dimension of the clusters (Muthukumar & Winter, 1986). The fractal dimensionality of the xanthan–Cr gel at the gelation threshold is estimated as $d_f = 1{\cdot}3$ from the observed relaxation exponent using the relation (Muthukumar, 1985):

$$d_f = 2n/(1-n) \tag{3}$$

This is intermediate between $d_f = 1{\cdot}0$ for gelatin gels (ter Meer *et al.*, 1990) on the one hand and $d_f = 1{\cdot}5$ and 1·78 for agar in the gel and molecularly dispersed states on the other hand (Burchard & Ross-Murphy, 1990). The observed d_f for the xanthan gels indicate elongated structures between the branching points, which is not unexpected because of the stiff double-helical structure. The authors therefore conclude that the observed relaxation exponent is physically reasonable in view of the xanthan chain rigidity and reports on the fractal dimensionality of other gels.

The detailed analysis above was justified only when there was no substantial change in G' and G'' over the duration of one frequency scan. When gelation was more rapid, as for instance with increasing Cr(III) concentration or higher T, this analysis did not as clearly reveal the crossover point as in Fig. 3(b). Determination of relaxation exponents and fractal dimensionalities as a function of temperature and concentration ratios was therefore not carried out. The subsequent analyses were therefore limited to the following two parameters of the crosslinking process: (1) the maximum gradient of the storage modulus, beyond the gel point versus time ($\Delta G'/\Delta t$) at one selected frequency ($\omega = 0{\cdot}157$/s); and (2) the time to reach the crossover point where G' equals G'' at the frequency $\omega = 0{\cdot}157$/s, which will be referred to as the gelation time, t_G.

Effect of xanthan concentration on gelation time and rate of gelation

The crosslinking process of xanthan in the concentration range 0·5–2·5 mg/ml with 5 mmol/liter $Cr(NO_3)_3$ at pH = 3·4 and at $T = 20°C$ was investigated over a period of 40 h. Equilibrium was not reached in all cases even after this time. Table 1 shows t_G, $(\Delta G'/\Delta t)$ and $G'(t = 40\ h)$ for the three polymer concentrations. The gelation time t_G is of the order of a few hours at $c = 0{\cdot}5$ mg/ml and decreases with increasing xanthan concentration, to about half an hour at 2·5 mg/ml. The inverse of the gelation time, t_G^{-1}, depends linearly on the xanthan concentration, and extrapolation to 0/min yields an intercept at $c_0 = 0{\cdot}35$ mg/ml. The same intercept, $c_0 = 0{\cdot}35$ mg/ml, was also found by extrapolation of the rate $\Delta G'/\Delta t$ versus xanthan concentration to $\Delta G'/\Delta t = 0$ Pa/h. This indicates a lower critical xanthan concentration needed for gelation.

Table 1. Influence of xanthan concentration on gelation kinetics[a]

Xanthan (mg/ml)	pH	t_G (h)	$G'(t = 40\ h)$ (Pa)	$(\Delta G'/\Delta t)_G$ (Pa/h)
0·5	3·4	3·25	3·6	0·08
1·0	3·4	1·60	35·0	0·26
2·5	3·4	0·45	60·0	0·74

[a] $[Cr(NO_3)_3]$ = 5 mmol/liter.

The apparent lower critical polymer concentration c_0 for gel formation is close to the overlap concentration c^* estimated from the experimentally determined $[\eta]$ to $c^* = 1{\cdot}4/[\eta] = 0{\cdot}33$ mg/ml. The numerical constant for relating c^* to $[\eta]$ was assumed to be 1·4 according to experimental determination of the overlap concentration of xanthan (Milas *et al.*, 1990; Stokke *et al.*, 1992). This indicated that chain overlap is a prerequisite for gelation, but should be confirmed using several samples with different molecular weights. Intramolecular crosslinking is expected to be a dominant process at $c < c_0$ in analogy with that reported for intramolecular crosslinking of polyacrylamide with Cr (Allain & Salome, 1990). The values of G' after 40 h indicate that an increase in polymer concentration leads to a stronger gel, i.e. the number of elastically active chains increases with increasing polymer concentration for a given concentration of chromium.

The rate of gelation increases with xanthan concentration. The correlation on a log–log scale indicates that $\Delta G'/\Delta t$ depends on the polymer concentration to the 1·25 ± 0·25 power. The observed coefficient is less than the characteristic second power dependence expected for a bimolecular rate-limiting process. Deviation from a second power dependence is most likely to be due to the few selected concentrations covering less than one decade. It should also be noted that the actual concentration range is close to the lower critical concentration c_0, a range where the interpretation of the observed power law coefficients is more complex (Ross-Murphy, 1991).

The effect of Cr(III) concentration on gelation

Figure 4 shows the experimentally determined t_G and $\Delta G'/\Delta t$ as a function of Cr(III) concentration for 1·25 mg/ml xanthan at pH 3·4 and at $T = 20°C$. Both t_G and $\Delta G'/\Delta t$ depend strongly on the concentration of

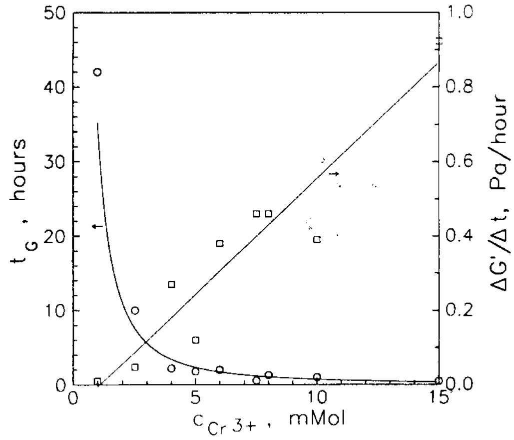

Fig. 4. The gelation time t_G (○) and rate of change in $G'(\omega = 0{\cdot}157\ \mathrm{rad/s})$ (□) at the gelation threshold versus chromium concentration for pH = 3·4 and 1·25 mg/ml xanthan. T = 20 °C.

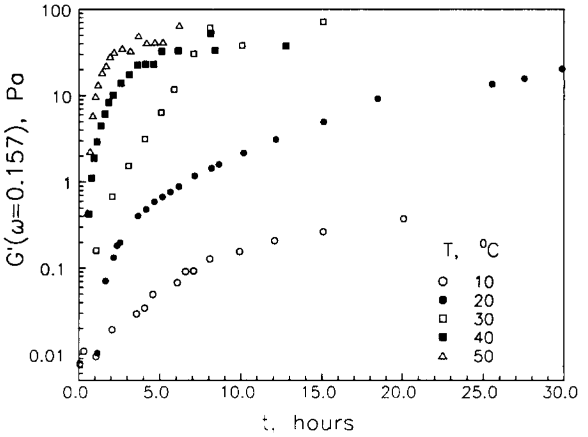

Fig. 5. Storage modulus $G'(\omega = 0{\cdot}157/\mathrm{s})$ versus reaction time after mixing at various temperatures for 1·25 mg/ml xanthan, 5 mmol/liter $Cr(NO_3)_3$, and pH 3·4.

chromic ions. Reducing the concentration from 15 to 1 mmol/liter results in an increase of t_G from about 0·5 h to 42 h at this temperature. The divergence of t_G and the intercept of $\Delta G'/\Delta t$ at 0 Pa/h versus c_{Cr} (Fig. 4) indicate a lower critical concentration of Cr(III) needed to induce gelation of about 1 mM $Cr(NO_3)_3$. This represents a minimum number of crosslinks necessary to change the viscous xanthan solution to a viscoelastic solid. The present estimate of an apparent lower critical Cr concentration accords with a previous paper (Lund *et al.*, 1988) which reports on a critical Cr(III) concentration of 1–2 mM for the crosslinking of xanthan solutions made from a commercial dried powder.

Prud'homme *et al.* (1983) studied gelation of hydrolyzed polyacrylamide (HPAM) using Cr(VI) in combination with a reducing agent and reported a power law dependence of $\Delta G'/\Delta t$ at the gelation threshold on c_{Cr} with a coefficient equal to 2·7. This was interpreted as at least dimeric chromium species constituting the ionic bridges in the crosslinked polymer gel. The present authors' data on crosslinking xanthan with Cr(III) yields a power law dependence of $\Delta G'/\Delta t$ on c_{Cr} with a coefficient of 1·7 ± 0·2. This coefficient is lower, but departs less from 2 than does the value of 2·7 reported for HPAM–Cr(VI) (Prud'homme *et al.*, 1983). The present observed value of 1·7 ± 0·2 thus suggests that dimeric ion bridges are effective in crosslinking the xanthan polymer.

Effect of temperature on xanthan–chromium gelation

Figure 5 shows $G'(\omega = 0{\cdot}157/\mathrm{s})$ versus time after combining the xanthan and chromium solutions at T = 10, 20, 30, 40 and 50 °C. The gelation is slow at 10 °C, with a relatively small increase within the first five hours, and a gel with $G'(\omega = 0{\cdot}157/\mathrm{s}) = 0{\cdot}5$ Pa is observed after about one day. Increasing the temperature shifts the time interval such that the largest changes are occurring earlier after mixing. Concomitant, an increase in $G'(\omega = 0{\cdot}157/\mathrm{s})$ for temperatures up to about 30 °C followed by a temperature independent plateau for T above 30 °C is observed (Fig. 5).

The gelation time t_G and $\Delta G'/\Delta t$ plotted versus temperature summarizes these effects (Fig. 6(a)). The gelation time is inversely related to the temperature, and apparently diverges when cooled below 10 °C. The parameter $\Delta G'/\Delta t$ is observed to be larger the higher the temperature in the range investigated. Figure 6(b) shows $G'(\omega = 0{\cdot}157/\mathrm{s})$ after one day versus temperature in the in-situ gelation experiments, in comparison to E versus temperature for 10 mg/ml xanthan–100 mM $Cr(NO_3)_3$ gel cylinders made by the dialysis method at room temperature and equilibrated to the measuring temperature for 1 h prior to the experimental determination of $E(T)$. While there is a parallel decline in E and $G'(t = 24\ \mathrm{h})$ above 30 °C, $G'(t = 24\ \mathrm{h})$ is markedly reduced when gelation is carried out below 25 °C. The observed increase in gelation rate observed upon increasing the temperature was of practical value in making it possible to make xanthan–Cr gel beads suitable for studying volume changes in various solvents (see above). It has also been suggested that the temperature dependence of $\Delta G'/\Delta t$ can be used in permeability modification of oil reservoirs (Fletcher *et al.*, 1991). Waterflooding previous to the gel treatment sets up a cold-front inside the reservoir formation. Subsequent injection of a gelling polymer solution is envisaged to have the crosslinking retarded while in the cold zone. A large increase in gelation rate is encountered on reaching the warmer parts deeper in the formation, thus yielding a selective placement of the gel just beyond the cold-front. Detailed matching of the temperature dependence of the gelation to the reservoir temperature jump (simulated to be up to 30 °C) is of prime importance in such applications. The influence of temperature on the kinetics of gelation will below be

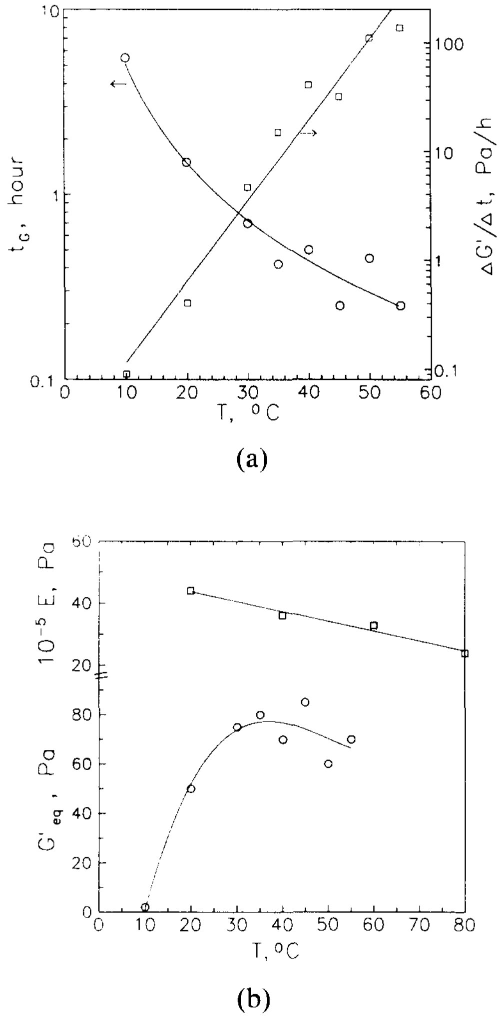

Fig. 6. (a) The gelation time t_G (○) and rate of change in $G'(\omega = 0{\cdot}157/s)$ (□) at the gelation threshold versus temperature for 1·25 mg/ml xanthan, 5 mmol/liter $Cr(NO_3)_3$ and pH = 3·4. (b) Apparent equilibrium storage modulus, $G'(t = 40$ h), of 1·25 mg/ml xanthan, 5 mmol/liter $Cr(NO_3)_3$ gelled *in situ* at the actual temperature (○) and modulus of elasticity of 10 mg/ml xanthan-100 mmol/liter $Cr(NO_3)_3$ gelled by dialysis at $T = 20$ °C and equilibrated at the actual temperature of measurement (□).

given an Arrhenius treatment yielding an apparent activation energy of the process.

Spectroscopy

Difference absorption spectroscopy was carried out on gels crosslinked directly in two sample cuvettes and using the same, e.g. 2·5 mg/ml xanthan and 10 mmol/liter $Cr(NO_3)_3$ (pH 3·4), concentrations in separate cuvettes in the reference beam. These difference spectra revealed a maximum in absorption at $\lambda = \lambda_{max} = 232$ nm at equilibrium ($t = 24$ h, $T = 25$ °C). Difference spectra of 5 mM chromium-5 mM sodium-acetate were observed to be similar to those of chromium-xanthan and have maxima at the same wavelength at equilibrium. The finding that the pairwise interactions acetate-Cr(III) and xanthan-Cr(III) yield similar difference absorption spectra, suggests that the carboxylic group of the glucuronic acid in the xanthan trisaccharide side chain (Jansson *et al.*, 1975) is the interaction site for Cr(III). Analogous results were reported (Allain & Salome, 1987, 1988, 1990) for the interaction between hydrolyzed polyacrylamide and Cr(III).

In attempting to determine simultaneously the number of crosslinks and the elasticity, the authors used the difference absorption at $\lambda = 250$ nm, ΔA ($\lambda = 250$ nm), for monitoring xanthan-Cr(III) interactions (Allain & Salome, 1988) to minimize influence of potential shifts in λ_{max}. ΔA ($\lambda = 250$ nm) of 5 mM $Cr(NO_3)_3$ was found to be proportional to the concentrations of $NaCH_3COO$ at equilibrium ($t = 24$ h, $T = 30$ °C) (Fig. 7, inset). Least square fit of a linear correlation yielded ΔA ($\lambda = 250$ nm) = 0·167 $[CH_3COO^-]$ − 0·019, when concentration is mmol/liter. This observed linear relation could be used in an attempt to correlate the observed difference absorption of the xanthan-Cr(III) gels to the concentration of crosslinks.

Figure 7 shows the correlation between the developing G' and ΔA ($\lambda = 250$ nm) in a 1·25 mg/ml xanthan, 5 mmol/liter $Cr(NO_3)_3$ gelling solution at $T = 30$ °C, pH 3·4. The data were extracted from the first 6·5 hours of gelation from parallel experiments carried out for the spectroscopical and rheological parts. We observe a characteristic non-linear relation between the change in ΔA ($\lambda = 250$ nm) and G'. Using the observed ΔA ($\lambda = 250$ nm) versus acetate concentration as calibration, the equilibrium ($T = 25$ °C, $t = 24$ h) values of ΔA ($\lambda = 250$ nm) for 1·25 mg/ml and 2·5 mg/ml xanthan-5 mM Cr(III) corresponded to 1·9 mM and 3·6 mM inter-

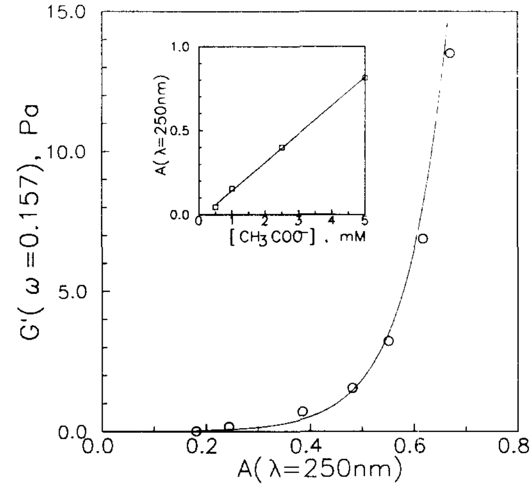

Fig. 7. Storage modulus $G'(\omega = 0{\cdot}157/s)$ versus ΔA ($\lambda = 250$ nm) (○) taken during gelation of 1·25 mg/ml xanthan, 5 mmol/liter $Cr(NO_3)_3$, pH 3·4 at $T = 30$ °C. Inset: ΔA ($\lambda = 250$ nm) versus acetic acid concentration 24 h after preparation of the solution (□).

acting carboxylic groups, respectively. This corresponds to 1·36 and 1·44 repeating units per interaction site at a total polymer concentration of 1·25 and 2·5 mg/ml, respectively. The total concentration of carboxylic groups was calculated from the polymer concentration and the molar mass of the xanthan repeating unit. The absorption data thus suggest that most of the carboxylic groups bind to the metal ion. The observed G' in view of the authors' previous estimates of molecular mass between junction points (Lund *et al.*, 1988) suggest that there are numerous ions interacting with the polymer which do not participate actively in forming ionic bridges. It is therefore uncertain whether the empirical correlation between the observed change in difference absorption due to xanthan–Cr(III) interaction and the resulting change in G' reflects changes in elasticity due to crosslink-density changes.

Estimation of apparent activation energies

The change of the gelation time t_G, and the rates $\Delta G'/\Delta t$ and ΔA (λ = 250 nm)/Δt with temperature suggest that these temperature effects can be described by an Arrhenius equation yielding activation energies (Fig. 8). The estimated apparent activation energies were E_a = 42, 102 and 43 kJ/mol based on t_G^{-1}, $\Delta G'/\Delta t$ and ΔA (λ = 250 nm)/Δt, respectively. These activation energies were estimated for c = 1·25 mg/ml and c_{Cr} = 5 mM. There is agreement between those E_a based on t_G and ΔA (λ = 250 nm)/Δt, whereas E_a based on $\Delta G'/\Delta t$ is about 2·5 times higher. This discrepancy is most likely due to the fact that t_G represents the same extent of reaction which can be related to the rate of change of the underlying process (the same one as the change in absorption represents), whereas the resulting $\Delta G'/\Delta t$ is also influenced by the cluster size distribution at the gelation threshold and the chain stiffness of the chains between junction points. The non-linear dependence of G' on ΔA (λ = 250 nm) during the gelation process (Fig. 7) illustrates that G' is not proportional to the number of interacting metal ions. Use of $\Delta G'/\Delta t(T)$ to estimate E_a will therefore not reflect the activation energy of the underlying crosslinking process.

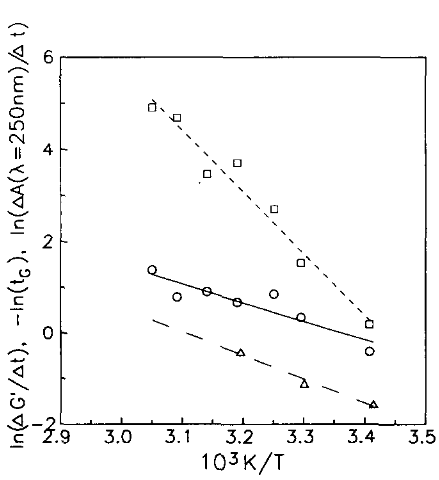

Fig. 8. Arrhenius plot of $-\ln t_G$ (O), ln ($\Delta G'/\Delta t$ (□) and ln (ΔA (λ = 250 nm)/Δt) (△) versus T^{-1}.

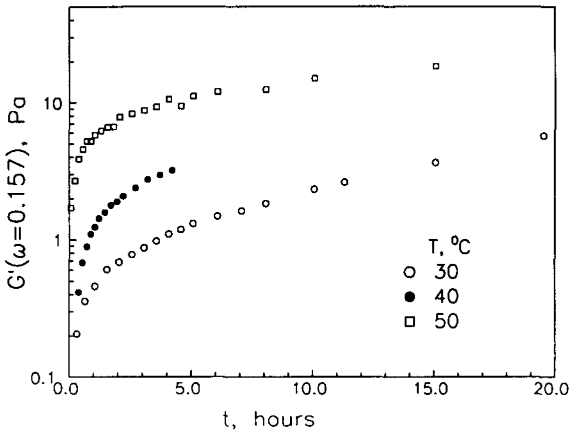

Fig. 9. Storage modulus $G'(\omega$ = 0·157/s) versus reaction time after mixing at various temperatures for 1·25 mg/ml xanthan, 2·5 mmol/liter $Al(NO_3)_3$ and pH = 4·0.

Kinetics of gelation in Al-crosslinked xanthan

Figure 9 shows $G'(\omega$ = 0·157/s) versus time of 2·5 mg/ml xanthan and 1·25 mM Al(III) solution at T = 30, 40 and 50 °C. By comparing these to the observed gelation kinetics in the xanthan–Cr(III) system (Fig. 4(a)), it is observed that the exchange of Cr(III) with Al increases the reaction rate. Concomitant to the increased rate of developing G' and decreasing t_G, it is also observed that the storage modulus after about one day is lower when using Al(III) than when using Cr(III) crosslinker. This agrees with the results of the experiments reported in Fig. 1. The apparent activation energy was estimated to be 108 and 190 kJ/mol when based on t_G^{-1} and $\Delta G'/\Delta t$, respectively. The activation energies estimated from experimentally determined t_G are, for the same reasons as discussed above for xanthan–Cr(III), preferable to those based on $\Delta G'/\Delta t$. In comparison with the Cr(III)-crosslinking of xanthan, we find that E_a increases from about 42 to 108 kJ/mol when Cr(III) is substituted for Al(III). The observed apparent activation energies, E_a = 42–100 kJ/mol and E_a = 108–190 kJ/mol for Cr- and Al-crosslinking of xanthan, are of the same order of magnitude as E_a = 70 kJ/mol reported for crosslinking HPAM with Cr(III) reduced from Cr(IV) (Jordan *et al.*, 1981), and E_a = 47 and 101 kJ/mol based on oscillatory and rotational rheological determination of gel points for xanthan–Cr(III) (Johnston & Hubbard, 1989).

CONCLUSIONS

Crosslinking of xanthan with Cr(III) gives generally higher gel strength at equilibrium than crosslinking with Al(III), as judged both from the elastic modulus of the gel cylinders and the shear modulus obtained in the kinetic experiments. Equally or more important than the selection of ion type on the gelation time are the reaction parameters, such as pH, concentration and, in particular, the temperature. The modulus of xanthan gel cylinders made by dialysis against Cr(III), Al(III) or Fe(III) metal ions at different pH values indicate that the ionic species need to be dimeric or higher oligomers to participate in the crosslinking reaction. The observed power law coefficient of the gelation time on the chromium concentration of 1·7 is in agreement with this. The rate of gelation, as determined both by rheological and spectroscopical methods, increases with temperature, and the temperature effect is larger in xanthan–Al(III) than in xanthan–Cr(III). Such a difference in temperature effects may allow more detailed matching between the gelling system and the reservoir temperature profile than when only one ion type is available.

ACKNOWLEDGMENT

This work is supported by Deminex Exchange program (H.N. and S.J.), and research grants from VISTA, a research cooperation between the Norwegian Academy of Science and Letters and Statoil, and from the Royal Norwegian Council for Scientific and Industrial Research (NTNF).

REFERENCES

Allain, C. & Salome, L. (1987). *Macromolecules*, **20**, 2957–8.

Allain, C. & Salome, L. (1988). In *Biological and Synthetic Polymer Networks*, ed. O. Kramer. Elsevier Applied Science, London, pp. 291–303.

Allain, C. & Salome, L. (1990). *Macromolecules*, **23**, 981–7.

Atkins, E. (1990). In *Novel Biodegradable Microbial Polymers*, ed. E.A. Dawes. Kluwer Academic Publishers, Dordrecht, NATO ASI Ser. E., pp. 371–86.

Baes, C.F. & Mesmer, R.E. (1976). *Hydrolysis of Cations*. John Wiley, New York.

Borchardt, J.K. (1989). *Am. Chem. Soc. Symp. Ser.*, **396**, 3–54.

Burchard, W. & Ross-Murphy, S.B. (eds) (1990). In *Physical Networks. Polymers and Gels*. Elsevier Applied Science, London, pp. 1–14.

Burrafato, G., Carminati, S., Bonaccorsi, F. & Lockhart, T.P. (1990). *Macromolecules*, **23**, 2402–6.

Chambon, F. & Winter, H.H. (1985). *Polym. Bull.*, **13**, 499–503.

Chambon, F. & Winter, H.H. (1987). *J. Rheol.*, **31**, 683–97.

Conway, M.W., Almond, A.W., Briscoe, J.E. & Harris, L.E. (1983). *J. Pet. Tech.*, Feb, 315–20.

Fletcher, A.J.P., Flew, S., Forsdyke, I.N., Morgan, J.C., Rogers, C. & Suttles, D. (1991). Proc. 6th European Symp. on Improved Oil Recovery, Stavanger, Norway, 21–23 May 1991, pp. 329–35.

Hejri, S., Green, D.W. & Willhite, G.P. (1989). SPE 19634 presented at the 64th Ann. Tech. Conf. and Exhib. of the Society of Petroleum Engineers, San Antonio, TX, 8–11 Oct. 1989.

Holzwarth, G. (1976). *Biochemistry*, **15**, 4333–9.

Hubbard, S., Roberts, L.J. & Sorbie, K.S. (1986). SPE/DOE 14595 presented at the SPE/DOE 5th Symp. on Enhanced Oil Recovery, Tulsa, OK, 20–23 April 1986.

Jansson, P.E., Kenne, L. & Lindberg, B. (1975). *Carbohydr. Res.*, **45**, 275–82.

Johnston, J. D. & Hubbard, S. (1989). Atomic Energy Establishment, Winfrith, Dorchester, Dorset, UK, report AEEW-R 2158.

Jordan, D.S., Green, D.W., Terry, R.E. & Willhite, G.P. (1981). SPE 10059 presented at the 56th Ann. Fall Conf. and Exhib. of the Society of Petroleum Engineers of AIME, San Antonio, TX, 5–7 Oct. 1981.

Lund, T., Smidsrød, O., Stokke, B.T. & Elgsaeter, A. (1988). *Carbohydr. Polymers*, **8**, 245–56.

Martinsen, A., Skjåk-Bræk, G. & Smidsrød, O. (1989). *Biotechnol. Bioeng.*, **33**, 79–89.

Meer, H.U. ter, Lips, A. & Busnel, J.-P. (1990). In *Physical Networks. Polymers and Gels*, ed. W. Burchard & S.B. Ross-Murphy. Elsevier Applied Science, London, pp. 253–69.

Menjivar, J.A. (1986). *Am. Chem. Soc. Symp. Ser.*, **213**, 209–26.

Mikkelsen, A., Stokke, B.T. & Elgsaeter, A. (1986). *Int. J. Bio-Medical Computing*, **17**, 215–26.

Milas, M., Rinaudo, M., Knipper, M. & Schuppiser, J.L. (1990). *Macromolecules*, **23**, 2506–11.

Moradi-Araghi, A., Beardmore, D.H. & Stahl, G.A. (1988). In *Water-Soluble Polymers for Petroleum Recovery*, ed. G.A. Stahl & D.N. Schulz. Plenum Press, New York, pp. 299–312.

Muthukumar, M. (1985). *J. Phys. Chem.*, **83**, 3161–8.

Muthukumar, M. & Winter, H.H. (1986). *Macromolecules*, **19**, 1284–5.

Prud'homme, R.K. & Uhl, J.T. (1984). SPE 12640 presented at the SPE/DOE 4th Symp. on Enhanced Oil Recovery, Tulsa, OK, 15–18 April 1984.

Prud'homme, R., Uhl, J.T., Poinsatte, J.P. & Halverson, F. (1983). *Soc. Pet. Eng. J.*, Oct., 804–8.

Ross-Murphy, S.B. (1991). *Carbohydr. Polymers*, **14**, 281–94.

Sato, T., Norisuye, T. & Fujita, H. (1984*a*). *Polymer J.*, **16**, 341–50.

Sato, T., Norisuye, T. & Fujita, H. (1984*b*). *Macromolecules*, **17**, 2696–700.

Scanlan, L.C. & Winter, H.H. (1991). *Macromolecules*, **24**, 47–54.

Shu, P. (1989). *Am. Chem. Soc. Symp. Ser.*, **396**, 137–44.

Skjåk-Bræk, G., Grasdalen, H. & Smidsrød, O. (1989). *Carbohydr. Polymers*, **10**, 31–54.

Stokke, B.T., Elgsaeter, A., Bjørnestad, E.Ø. & Lund, T. (1992). *Carbohydr. Polymers*, **17**, 209–220.

Troll, M., Dill, K.A. & Zimm, B.H. (1980). *Macromolecules*, **13**, 436–8.

Winter, H.H. & Chambon, F. (1986). *J. Rheol.*, **30**, 367–82.

Zhang, L., Takematsu, T. & Norisuye, T. (1987). *Macromolecules*, **20**, 2882–7.